J Physiol Sci (2010) 60:195–204
DOI 10.1007/s12576-010-0085-z

ORIGINAL PAPER

Voltage-gated Ca^{2+} channel mRNAs and T-type Ca^{2+} currents in rat gonadotropin-releasing hormone neurons

Nobuyuki Tanaka · Hirotaka Ishii · Chengzhu Yin · Makiko Koyama · Yasuo Sakuma · Masakatsu Kato

Received: 9 December 2009 / Accepted: 5 January 2010 / Published online: 26 January 2010

Abstract Gonadotropin-releasing hormone (GnRH) neurons play a pivotal role in the neuroendocrine regulation of reproduction. We have previously reported that rat GnRH neurons exhibit voltage-gated Ca^{2+} currents. In this study, oligo-cell RT-PCR was carried out to identify subtypes of the α_1 subunit of voltage-gated Ca^{2+} channels in adult rat GnRH neurons. GnRH neurons expressed mRNAs for all five types of voltage-gated Ca^{2+} channels. For T-type Ca^{2+} channels, α_{1H} was dominantly expressed in GnRH neurons. Electrophysiological analysis in acute slice preparations revealed that GnRH neurons from adult rats exhibited T-type Ca^{2+} currents with fast inactivation kinetics ($\sim$20 ms at $-$30 mV) and a time constant of recovery from inactivation of $\sim$0.6 s. These results indicate that rat GnRH neurons express subtypes of the α_1 subunit for all five types of voltage-gated Ca^{2+} channel, and that α_{1H} was the dominant subtype in T-type Ca^{2+} channels.

Keywords GnRH neurons · Ca^{2+} channels · T-type Ca^{2+} channels · Patch clamp · RT-PCR

Abbreviations

EGFP	Enhanced green fluorescent protein
GnRH	Gonadotropin-releasing hormone
DBB	Diagonal band of Broca
OVLT	Organum vasculosum of the lamina terminalis
mPOA	Medial preoptic area
ACSF	Artificial cerebrospinal fluid
TEA-Cl	Tetraethylammonium chloride
4AP	4-Aminopyridine

N. Tanaka · H. Ishii · C. Yin · M. Koyama · Y. Sakuma · M. Kato (✉)
Department of Physiology, Nippon Medical School, Sendagi 1, Bunkyo, Tokyo 113-8602, Japan
e-mail: mkato@nms.ac.jp

Introduction

Gonadotropin-releasing hormone (GnRH) neurons play a pivotal role in the neuroendocrine regulation of reproduction. Thus, the question arises as to how cell excitability of GnRH neurons is regulated. Both intrinsic and extrinsic mechanisms are involved in determining the membrane potential and firing pattern. We have previously investigated the intrinsic properties of rat GnRH neurons, and revealed the presence of all five types of voltage-gated Ca^{2+} currents [1, 2] and two types of Ca^{2+}-activated K^+ currents, namely SK and BK currents [2, 3]. In the present study, we further investigated the voltage-gated Ca^{2+} channels by means of their molecular biology and electrophysiology.

Voltage-gated Ca^{2+} channels are involved in the control of cell excitability and also mediate Ca^{2+} influx, thereby regulating Ca^{2+}-dependent cellular processes such as contraction, secretion, and gene expression [4, 5]. The voltage-gated Ca^{2+} channels are classified into low-voltage-activated Ca^{2+} channels (T-type channels) and high-voltage-activated Ca^{2+} channels (L, N, P/Q, and R-type channels). Rat GnRH neurons possess all five types of voltage-gated Ca^{2+} currents [1, 2]. One characteristic is that R-type Ca^{2+} currents contribute more than 60% to the total Ca^{2+} current in neonatal rat GnRH neurons and more than 40% in adult rat GnRH neurons, suggesting that generation of Ca^{2+} spikes is mainly mediated through R-type Ca^{2+} channels in the soma and dendrites [6]. Two reports have been published on the Ca^{2+} currents in mouse

GnRH neurons. In one report, the proportions of R-type Ca^{2+} currents are 8–15% in mouse GnRH neurons and the proportions of T-type Ca^{2+} currents are negligible [7]. However, the other report suggested the presence of T-type Ca^{2+} currents in mouse GnRH neurons [8]. Recently, Zhang et al. [9] reported that mouse GnRH neurons express all three α_1 subunits for T-type Ca^{2+} channels and that their expression level is modulated by 17β-estradiol (E2). These reports led us to investigate which subtypes of T-type Ca^{2+} channels are expressed in rat GnRH neurons. Three subtypes have been identified, namely Cav3.1 (α_{1G}), Cav3.2 (α_{1H}), and Cav3.3 (α_{1I}) channels [4, 10–12]. Each subtype exhibits distinct kinetics and Ni^{2+} sensitivity [4, 13]. The striking differences among these three subtypes are that the recovery time course from inactivation is rapid in α_{1G} and slower in α_{1H} and α_{1I}, and that inactivation is rapid in α_{1G} and α_{1H} but slower in α_{1I} [4, 14, 15]. Ni^{2+} sensitivity is high (IC_{50}, 12 μM) in α_{1H} and low ($IC_{50} > 200$ μM) in α_{1G} and α_{1I} [4, 13]. Consequently, expression of the different subtypes must affect cell excitability differently.

In this study, we investigated mRNA expression for the voltage-gated Ca^{2+} channels using multi-cell RT-PCR and performed electrophysiological analyses of the T-type Ca^{2+} currents in rat GnRH neurons in acute slice preparations. We found that rat GnRH neurons expressed mRNAs for all five types of voltage-gated Ca^{2+} channels, and that α_{1H} was dominantly expressed for the T-type Ca^{2+} channel. There were no sex differences in expression of the mRNAs and no difference with regard to estrous cycle stage for the dominance of α_{1H} expression.

A preliminary report of some of our findings has been published previously in abstract form [16].

Materials and methods

Animals

All experiments were performed after obtaining approval from the Nippon Medical School Animal Care Committee. Transgenic rats expressing enhanced green fluorescent protein (EGFP) under the control of the GnRH promoter [1] were used. The rats had free access to water and chow, and were maintained under a 14-h light/10-h dark cycle. Rats aged 2–3 months (adult) were used for electrophysiological experiments and multi-cell RT-PCR analyses.

Preparation of slices

Coronal brain slices (200-μm thick) containing the medial septum, diagonal band of Broca (DBB), organum vasculosum of the lamina terminalis (OVLT), and medial preoptic area (mPOA) were prepared from male and female rats. Rats were decapitated under ether anesthesia, and their brains were quickly removed and immersed in an ice-cold oxygenated (100% O_2) cutting solution comprising (mM) 2.5 KCl, 1.25 Na_2HPO_4, 0.6 $NaHCO_3$, 0.5 $CaCl_2$, 7 $MgCl_2$, 10 HEPES, 7 glucose, 248 sucrose, 1.3 ascorbic acid, and 3 Na pyruvate (pH 7.4, 290 mOsm). The brains were cut into blocks, glued with cyanoacrylate to the chilled stage of a Vibratome VIB3000 (Vibratome, St Louis, MO, USA) and sliced. The slices were transferred to and maintained in a chamber containing an oxygenated artificial cerebrospinal fluid (ACSF) consisting of (mM) 137.5 NaCl, 2.5 KCl, 1.25 Na_2HPO_4, 0.6 $NaHCO_3$, 10 HEPES, 2 $CaCl_2$, 2 $MgCl_2$, and 10 glucose (pH 7.4) at room temperature for 30 min or more.

Preparation of dissociated cells

The brains were excised from rats under ether anesthesia in the afternoon (12:00). The medial septum, DBB, OVLT, and mPOA were cut out with razors and surgical blades. The sections were minced and treated with papain (21U/ml; Funakoshi, Tokyo, Japan) for 50 min at 30°C with Dulbecco's modified Eagle's medium (Sigma, St Louis, MO, USA). Tissues were triturated with a 5-ml plastic pipette after several washes with modified Eagle's medium (Invitrogen, Grand Island, NY, USA). Cell suspensions were applied to a discontinuous Percoll (Amersham Biosciences, Uppsala, Sweden) density gradient composed of 1.0, 1.023, and 1.078 g/ml layers, and centrifuged. The cells were obtained from the middle layer and EGFP-positive (GnRH) cells were harvested with a glass suction pipette for RT-PCR analysis. For electrophysiological experiments, the cells were plated on poly-lysine-coated coverslips and incubated overnight in neurobasal-A medium (Invitrogen, Grand Island, NY, USA) supplemented with 0.5 mM L-glutamine, B-27 (Invitrogen), and 5 ng/ml basic FGF (Invitrogen) at 37°C. The estrous cycle stage was determined on the day of sacrifice.

Electrophysiology

A List EPC-9 patch-clamp system (Heka Electronic, Lambrecht/Pfalz, Germany) was used for the recordings and data analyses. T-type Ca^{2+} currents were recorded by means of the whole-cell patch clamp configuration at 32°C. Each slice was transferred to the recording chamber, kept submerged, and continuously superfused with oxygenated ACSF at a rate of 3 ml/min. The slice was viewed under an upright fluorescence microscope (BX50; Olympus, Tokyo, Japan). For whole-cell recordings, pipettes were fabricated from borosilicate glass capillaries and had a resistance of 4–5 MΩ. The pipette solution consisted of (mM) 130 Cs-gluconate, 10 EGTA, 10 HEPES, 0.3 $MgCl_2$, and 2 Mg-ATP (pH 7.3, 280 mOsm). The T-type Ca^{2+} currents

were recorded using TEA/Ca^{2+} ACSF consisting of (mM) 2 NaCl, 103 tetraethylammonium chloride (TEA-Cl), 5 CsCl, 10 $CaCl_2$, 0.8 $MgCl_2$, 10 glucose, 20 HEPES, 0.6 $NaHCO_3$, and 10 4-aminopyridine (4AP) (pH 7.4, 290 mOsm). Under these recording conditions nearly all Na^+ and K^+ currents were eliminated. Thus, the Ca^{2+} currents were isolated. Positive pressure was applied to the pipette and the pipette was then targeted at the GnRH neuron identified by EGFP fluorescence. After the cell was reached, the positive pressure was removed and negative pressure was applied to seal (seal resistance, >3 GΩ) and break the patch membrane. The currents were filtered at 2.3 kHz, digitized at 10 kHz, and stored. The series resistance was electronically compensated by 70%. Data were acquired when the series resistance was stable and <30 MΩ. The cell capacitance was 17.31 ± 3.95 pF (mean ± SD, $n = 190$). Capacitative and leak currents were subtracted by the p/n procedure, and the liquid junction potential was not compensated. The holding potential was −50 mV. To measure the activation of T-type Ca^{2+} currents, 100-ms test pulses (−80 up to −20 mV in 5 or 10-mV increments), preceded by a 2-s prepulse of −100 mV to fully deactivate the T-type channels, were applied at 0.1 Hz. The inactivation time constant was determined by exponential fitting as shown in Fig. 3d. To measure the steady-state inactivation of the T-type Ca^{2+} currents, 2-s prepulses (−100 up to −40 mV in 5-mV increments) followed by a test pulse (−20 mV) were applied at 0.1 Hz. The data were normalized by the value obtained for the −20 mV pulse for the activation and by the value at −100 mV for the steady-state inactivation. The recovery time course of the T-type Ca^{2+} currents was determined using a voltage sequence consisting of 2-s depolarizing prepulses to −30 mV followed by a −100-mV pulse of variable length (0.01–2 s) and a test pulse to −20 mV at 0.1 Hz. In some experiments, the T-type channel blocker Ni^{2+} (100 μM) was used at the end of the recordings to confirm the T-type currents. In current-clamp experiments, ACSF and pipette solution consisting of (mM) 90 K-gluconate, 40 KCl, 10 EGTA, 10 HEPES, 0.3 $MgCl_2$, and 2 Mg-ATP (pH 7.3, 280 mOsm) were used. The membrane potentials were kept at −55 to −60 mV. Rebound action potentials were elicited with 1-s hyperpolarizing current pulse.

Multi-cell RT-PCR

Coronal slices (200-μm thick) were prepared as described above. Each slice was transferred to the recording chamber, kept submerged, and continuously superfused with oxygenated ACSF at a rate of 3 ml/min. The slice was viewed under an upright fluorescence microscope (BX50; Olympus). Pipettes of 1–2 MΩ (inner tip diameter, 4–6 μm) were fabricated from glass capillaries baked at 200°C for 5 h. Each pipette was filled with 5 μl of an autoclaved solution comprising (mM) 150 KCl, 3 $MgCl_2$, 5 EGTA and 10 HEPES (pH 7.2, 270 mOsm). The cytoplasmic contents were harvested from 5 GnRH neurons under visual control, and pooled in a thin-walled PCR tube containing an RNase inhibitor (RNasin *Plus*; Promega, Madison, WI, USA). In some experiments, GnRH neurons were harvested from acutely-dispersed preparation. The harvested contents were heated with random hexamer primers (Promega) at 95°C for 5 min and then cooled on ice for 1 min. The RT mixture (50 μl) contained cytoplasmic contents from 5 cells, 1× RT buffer, 1 mM dNTP mixture, 500 ng random hexamer primers, 40 U fresh RNasin *Plus*, and 200 U ReverTra *Ace* (M-MLV reverse transcriptase, RNase H (−); Toyobo, Osaka, Japan). Reverse transcription was carried out at 30°C for 10 min and then at 42°C for 45 min. After stopping the reaction by heating at 75°C for 15 min, the reaction mixture was treated with RNase H (Takara Bio, Shiga, Japan) at 37°C for 30 min and stored at −80°C until use. To confirm successful cDNA synthesis from the cytoplasmic contents of the GnRH neurons, a one-round PCR amplification of GnRH mRNA transcripts was performed using 2-μl aliquots of the RT mixture as a template. For voltage-gated calcium channel α_1 subunits, a two-round PCR amplification was performed using 10-μl aliquots of the RT mixture as a template for the first-round PCR and 0.5-μl aliquots of the first-round PCR solution as a template for the nested second-round PCR. The PCR conditions were 94°C for 2 min, 28 cycles of 94°C for 30 s, 57°C for 20 s, and 72°C for 30 s, and, finally, 72°C for 5 min. The PCR mixture (50 μl) contained template DNA, 1× PCR buffer, 0.2 mM dNTP mixture, 0.2 μM forward and reverse primers, and 1.2 U Blend Taq polymerase (Toyobo). The primer sequences are shown in Table 1. The PCR products (5 μl) were separated by electrophoresis in 2% agarose gels, and visualized by ethidium bromide staining under UV irradiation. Gel images were captured using a FAS-III system (Toyobo). The PCR products were confirmed by DNA sequencing. Briefly, the PCR products were extracted from the agarose gels using a Wizard SV Gel and PCR clean-up system (Promega), and cloned into pGEM-T-Easy vectors (Promega). Sequencing reactions were performed using a BigDye terminator v3.1 cycle sequencing kit (Applied Biosystems, Foster City, CA, USA). Fluorescence signals were detected using an ABI Prism 310 genetic analyzer (Applied Biosystems).

Statistical analysis

Data were obtained from at least three independent experiments, and expressed as mean ± SEM unless otherwise indicated. Fisher's exact probability test and a *t* test were used for statistical analysis. The significance level was set at $P < 0.05$.

Table 1 Primer sequences and amplicon lengths

Type	Gene		Direction	Primer sequence (5′ to 3′)	Product size (bp)	Accession number
L-type	α_{1S}	1 st PCR	Forward	5′-GGCCATGCTCCCCCTGTT-3′	210	AB374360[a]
			Reverse	5′-CACTCGCTGCCGTTGATGG-3′		
		2nd PCR	Forward	5′-ACATCGCCCTGCTCGTCCTCT-3′	190	
			Reverse	5′-CACTCGCTGCCGTTGATGG-3′		
	α_{1C}	1st PCR	Forward	5′-ACAGCGGAAGCGGCAGCAGTAT-3′	336	NM_012517
			Reverse	5′-AGGTAAGCGTTGGGGTGGAAGAGT-3′		
		2nd PCR	Forward	5′-AGCGGAAGCGGCAGCAGTATG-3′	233	
			Reverse	5′-GGAGTTGGTGGCGTTGGAGTCAT-3′		
	α_{1D}	1st PCR	Forward	5′-ATGGTCCCCCTCCTCCACATAG-3′	346	NM_017298
			Reverse	5′-ATGGCCACTCCCATCCTATCG-3′		
		2nd PCR	Forward	5′-GGTCCCCCTCCTCCACATAGC-3′	212	
			Reverse	5′-CGACCCAGCCGCTCCTACATT-3′		
	α_{1F}	1st PCR	Forward	5′-AAGACGGAGGACTCAGCACAACAA-3′	387	NM_053701
			Reverse	5′-CTGAACAGCCCGACTACAACGAT-3′		
		2nd PCR	Forward	5′-GCACAACAAGCACAAGACCGTAGT-3′	320	
			Reverse	5′-GAATGTAGGCGCTGGGATGGA-3′		
P/Q-type	α_{1A}	1st PCR	Forward	5′-GCCCAACAACGGCATCACTCA-3′	250	NM_012918
			Reverse	5′-AAAAGCCCTTCGGTTCTCTACACG-3′		
		2nd PCR	Forward	5′-GCCCAACAACGGCATCACTCA-3′	193	
			Reverse	5′-ACCCAGCACAAGGTTCAGCATAA-3′		
N-type	α_{1B}	1st PCR	Forward	5′-TGTACAACCCCATCCCAGTCAAG-3′	400	NM_147141
			Reverse	5′-AGGGTGCGCAGATCAAAGTCAGTT-3′		
		2nd PCR	Forward	5′-TGTACAACCCCATCCCAGTCAAG-3′	266	
			Reverse	5′-GCCCGCCTCGAAGCAAAAG-3′		
R-type	α_{1E}	1st PCR	Forward	5′-CCTCCGGGCTGTGCGTGTC-3′	292	NM_019294
			Reverse	5′-GGGGCCGATCCAGTCCTTAC-3′		
		2nd PCR	Forward	5′-TTCTGCTCTTCTTTGCCATTCTCAT-3′	177	
			Reverse	5′-GGCCGATCCAGTCCTTACATTCATA-3′		
T-type	α_{1G}	1st PCR	Forward	5′-GCATGCGCATTCTCGTCACATTA-3′	394	NM_031601
			Reverse	5′-TCGCCCGCAGAGCAGTTG-3′		
		2nd PCR	Forward	5′-ATGCGCATTCTCGTCACATTACT-3′	216	
			Reverse	5′-GGGGCTCTCGTCCTCATTCTCT-3′		
	α_{1H}	1st PCR	Forward	5′-ATCTGCTCCTCCCGCCGTGAC-3′	428	NM_153814
			Reverse	5′-AGCTGGTTTTCCCTTTGCTTTGT-3′		
		2nd PCR	Forward	5′-ATCTGCTCCTCCCGCCGTGAC-3′	275	
			Reverse	5′-ACCCAGCCCTCCAGTGTGATG-3′		
	α_{1I}	1st PCR	Forward	5′-CCTCTCAAAGCCATCAACCGTGTA-3′	367	NM_020084
			Reverse	5′-GCCCCGCCCCGAAGTCATA-3′		
		2nd PCR	Forward	5′-CTTCTTCATCTTCGGCATCATTGG-3′	262	
			Reverse	5′-CCCGCCCCGAAGTCATACAC-3′		
	GnRH		Forward	5′-ACTGATGGCCGCTGTTGTTCT-3′	256	NM_012767
			Reverse	5′-CTTCTTCTGCCCAGCTTCCTCTTCA-3′		

Each forward and reverse primer was designed on different exons to distinguish the amplification of target cDNA from that of genomic DNA

[a] The sequence for the α_{1S} subunit was newly determined and registered (accession number: AB374360)

Chemicals

4AP and TEA-Cl were purchased from Wako Junyaku (Osaka, Japan).

Results

Transcripts for rat voltage-gated Ca^{2+} channels in GnRH neurons

To determine the expression patterns of the mRNAs encoding voltage-gated Ca^{2+} channels in rat GnRH neurons, multi-cell RT-PCR analyses were performed using specific primers for L-type (α_{1S}, α_{1C}, α_{1D} and α_{1F}), P/Q-type (α_{1A}), N-type (α_{1B}), R-type (α_{1E}), and T-type (α_{1G}, α_{1H} and α_{1I}) subunits of Ca^{2+} channels and GnRH. In GnRH neurons from adult rats, the R-type channel mRNA was detected in all samples examined (Figs. 1, 2a, b). The N and P/Q-type channel mRNAs were positive in ~50% of the samples. Among the L-type channel mRNAs, α_{1C} (Cav1.2) and α_{1D} (Cav1.3) were positive in ~20 and ~40% of the samples, respectively, and no positive bands were detected for α_{1S} and α_{1F}. Among the T-type channel mRNAs, α_{1H} (Cav3.2) was dominant (40–60% of the samples). α_{1G} (Cav3.1) and α_{1I} (Cav3.3) were positive in ~10% of the samples. α_{1C} and α_{1G} were negative in the male DBB/OVLT. α_{1I} was negative in the female mPOA. GnRH was positive in all reactions. Regarding the expression patterns of the Ca^{2+} channel subunit mRNAs, there were no sex differences and no differences between the DBB/OVLT and mPOA, except for α_{1C}, α_{1G}, and α_{1I} (Fig. 2a, b). The dominant expression of α_{1H} was affected by neither sex nor estrous cycle stage (Fig. 2c).

Activation and steady-state inactivation of the T-type Ca^{2+} currents

T-type currents are low-voltage-activated Ca^{2+} currents that have unique kinetics among the voltage-gated Ca^{2+} currents. We analyzed the T-type currents in acute slice preparations from GnRH-EGFP rats. To measure the activation of the T-type Ca^{2+} currents, test potentials (−80 to −20 mV) were applied and the peak current at each potential was measured (Figs. 3a, 4a). The T-type Ca^{2+} channel blocker Ni^{2+} (100 μM) blocked the inward currents (Fig. 3c), indicating the presence of T-type currents (Fig. 3d). In GnRH neurons from adult rats, the peak current densities at −30 mV were 15.0 ± 5.3 pA/pF ($n = 8$) in females and 15.8 ± 2.1 pA/pF ($n = 10$) in males. The inactivation time constants of the T-type currents at −30 mV were 22.3 ± 1.7 ms ($n = 8$) in females and 19.8 ± 1.4 ms ($n = 9$) in males. These values correspond to the currents through channels composed of α_{1G} or α_{1H} [4, 14, 15]. The inactivation time constants were voltage-dependent, and decreased by 70% in females and 61% in males between −45 and −25 mV (Fig. 3e). There were no statistically significant differences in the current density and inactivation time constant with regard to sex.

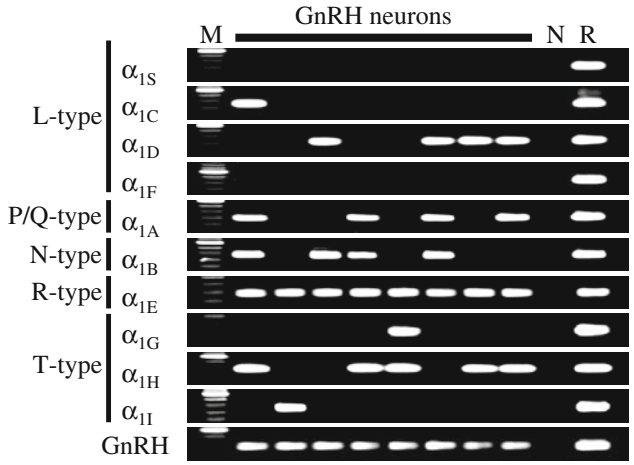

Fig. 1 Multi-cell RT-PCR analyses of mRNAs encoding voltage-gated Ca^{2+} channel α_1 subunits in adult rat GnRH neurons. Cytosols harvested from five GnRH neurons in slice preparation were pooled and reverse-transcribed to generate cDNAs, which were then subjected to PCR amplification with specific primers. The amount of cDNA used for each PCR corresponds to one cell for the Ca^{2+} channel α_1 subunits and 0.2 cells for GnRH. *M* 100-bp marker ladder, *N* cytosols without reverse transcriptase, *R* reference tissues (hypothalamus for α_{1A-E}, α_{1G-H}, and GnRH; skeletal muscle for α_{1S}; eye for α_{1F})

The T-type currents began to be activated around −60 mV (Fig. 4a, c). In steady-state inactivation experiments, the T-type currents were half-inactivated at around −55 mV and fully inactivated at −30 mV (Fig. 4b, c). Therefore, there was a small window T-type Ca^{2+} current between −60 and −30 mV, indicating a small proportion of the channel is active in these voltages. The voltages are not corrected for the liquid junction potential. There were no sex differences in the voltage-dependent activation and steady-state inactivation.

Recovery time constants of the T-type Ca^{2+} currents

The recovery time constants ranged from 0.45 to 0.75 s with a median of 0.61 s in males and from 0.25 to 1.32 s with a median of 0.75 s in females. All the values except one among the females were slower than 0.45 s. Exponential regression analyses of the pooled data produced recovery time constants of 0.59 s ($n = 5$) in males and 0.65 s ($n = 6$) in females (Fig. 5). These values correspond to the currents through channels composed of α_{1H} or α_{1I} [4, 14, 15]. There were no sex differences in the recovery time

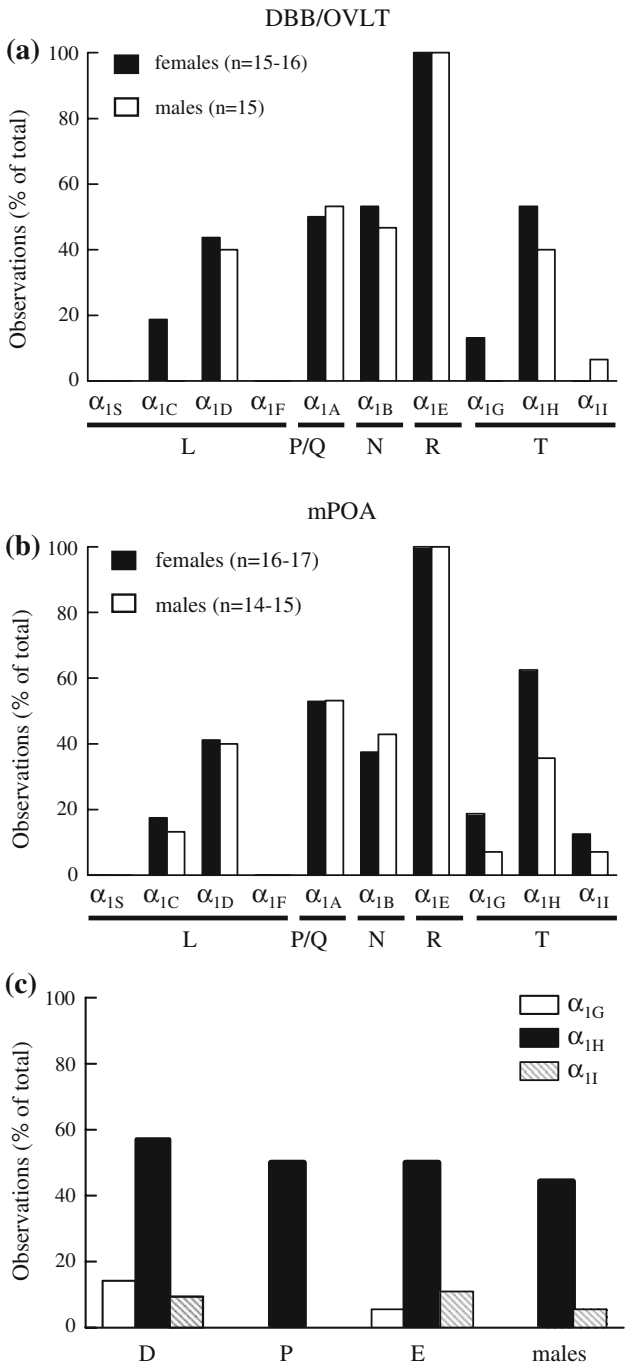

Fig. 2 Expression patterns of voltage-gated Ca^{2+} channel α_1 subunits in male and female rat GnRH neurons. The appearance of positive bands in the RT-PCR analyses is shown as a percentage of the total reactions for each subunit. **a**, **b** Results were obtained with GnRH neurons harvested from DBB/OVLT slices and mPOA slices. The numbers of reactions are indicated in the figures. **c** Expression patterns of α_1 subunits for T-type Ca^{2+} channel in estrous cycle stages and males. *D* diestrus ($n = 21$), *P* proestrus ($n = 18$), *E* estrus ($n = 18$), males ($n = 18$). Cells were harvested from an acutely dispersed preparation

courses from the inactivation produced by a 2-s pulse of −30 mV.

Rebound action potential

In current-clamp recordings rebound action potential was generated by a hyperpolarizing current pulse both in dissociated GnRH neurons and in the neurons in slice preparation (Fig. 6). The rebound action potential was blocked by 100 μM Ni^{2+}, indicating an involvement of T-type Ca^{2+} channels. As shown in Fig. 6, only a single rebound action potential but not a burst of action potentials was observed.

Discussion

These results demonstrated that GnRH neurons from adult rats express α_1 subunit mRNAs for all types of voltage-gated Ca^{2+} channels, namely L, N, P/Q, R, and T-type channels. These results are consistent with our previous report on the voltage-gated Ca^{2+} currents in rat GnRH neurons [1, 2]. Qualitatively similar Ca^{2+} currents have also been reported in mouse GnRH neurons [7, 8].

This study also revealed that rat GnRH neurons express α_{1D} mRNA and, to a lesser extent, α_{1C} mRNA, but not α_{1S} and α_{1F} mRNAs, for the L-type Ca^{2+} channels. Therefore, the L-type Ca^{2+} channels in rat GnRH neurons are mainly composed of the neuroendocrine subunit type (α_{1D}) and are devoid of the skeletal muscle subunit type (α_{1S}) and retina subunit type (α_{1F}) [5]. For T-type Ca^{2+} channels, α_{1H} was dominant in GnRH neurons of adult rats. The dominant expression of α_{1H} was not affected by either sex or estrous cycle stage. In contrast with our results, both α_{1H} and α_{1I} are reported to be dominant in GnRH neurons from ovariectomized E2-treated mice [9]. A high-dose of E2 elevates expression of α_{1H} and α_{1I} in the morning, and suppresses expression of α_{1H} without affecting that of α_{1I} in the afternoon [9]. Thus, there is a clear difference in the expression of α_{1I} between mouse and rat GnRH neurons. This may be because of a species difference. Concerning the effect of E2, expression of α_{1H} was still dominant in the afternoon of proestrus, during which E2 level is high, in rat GnRH neurons, whereas that is suppressed in E2-treated mice. The precise cause of this discrepancy is not known, although it may be because of a species difference and/or the different experimental design. The subtype specificity of the T-type Ca^{2+} channels in rat GnRH neurons was also confirmed by kinetic analyses of the T-type Ca^{2+} currents. In the GnRH neurons from adult rats, the inactivation time

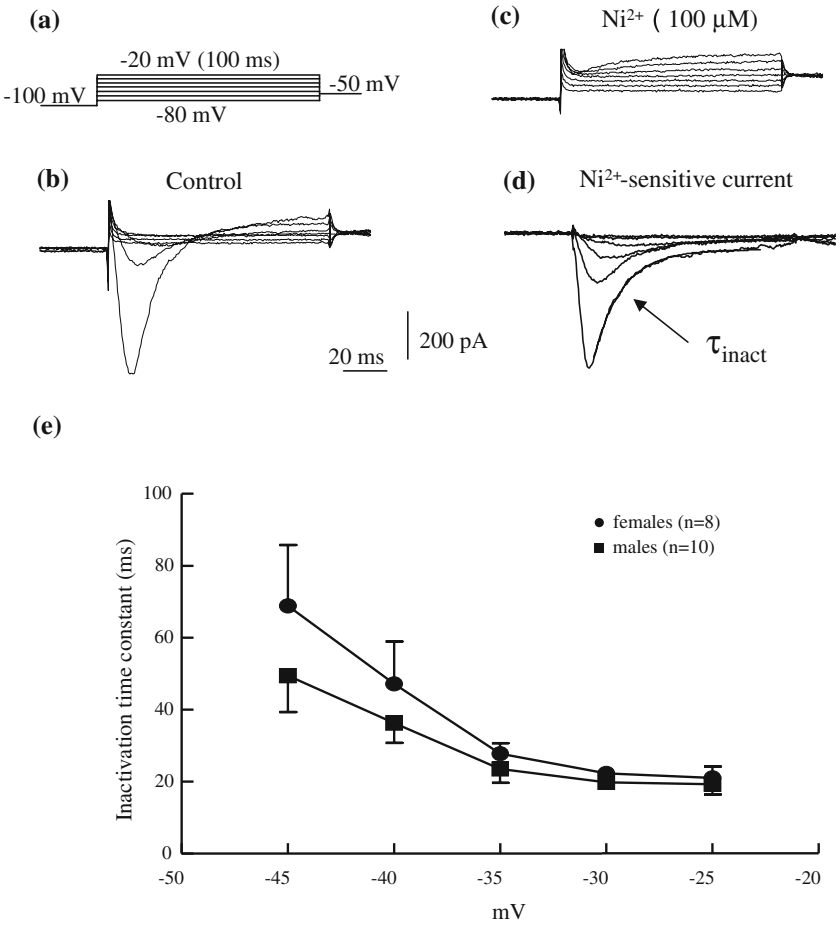

Fig. 3 T-type Ca^{2+} currents. **a** Voltage sequence. Test pulses (100 ms, −80 up to −20 mV in 10-mV increments), preceded by a 2-s prepulse of −100 mV to fully deactivate the T-type channels, were applied at 0.1 Hz. **b–d** Representative current traces; the capacitative and leak currents were not subtracted in (**b**) and (**c**). The T-type Ca^{2+} channel blocker Ni^{2+} (100 µM) blocks the inward currents (**c**), suggesting the presence of T-type currents, based on the difference currents (**d**) between the control currents (**b**) and currents with Ni^{2+} (**c**). The inactivation time constant was determined by exponential fitting as shown in (**d**). **e** Variation of inactivation time constant with command voltage. Data represent means ± SEM. *Upper* or *lower error bars* are shown for clarity. (The voltages are not corrected for liquid junction potential in this figure or in Figs. 4–6)

constant was ∼20 ms at −30 mV, suggesting the expression of α_{1G} and/or α_{1H} but not α_{1I} [10, 15]. The recovery time constant was ∼0.6 s, indicating the expression of α_{1H} and/or α_{1I} [14]. Taken together, these results indicate that the T-type Ca^{2+} channels in GnRH neurons from adult rats are mainly composed of α_{1H} both in males and females.

Regarding the physiological implications, T-type Ca^{2+} channels are most likely to be involved in the regulation of the intracellular Ca^{2+} concentration and the generation of Ca^{2+} spikes. Our results reveal that the window current of the T-type channels in rat GnRH neurons ranged from −60 to −30 mV. These voltages are not corrected for the liquid junction potential of ∼10 mV [17, 18]. It is also to be noted that the extracellular Ca^{2+} concentration was 10 mM in our experiments, except current-clamp recordings. High concentration (10 mM) of Ca^{2+} exerts the surface charge shielding effect. Consequently, a certain proportion of the T-type Ca^{2+} channels must be active at the resting potential of ∼−60 mV, thereby contributing to cellular Ca^{2+} homeostasis. No other voltage-gated Ca^{2+} channels are active at this voltage [1]. For example, the activation threshold of R-type Ca^{2+} currents is −40 mV (without correction for the liquid junction potential) [1]. The resting Ca^{2+} influx through the T-type Ca^{2+} channels may activate the Ca^{2+}-dependent cellular machineries, for example the SK channels [2]. Indeed, a small proportion of SK channels may be active at the resting membrane potential, because application of the SK channel blocker apamin was reported to depolarize mouse GnRH neurons [19].

T-type Ca^{2+} channels are also expressed in somatodendritic membranes [6]. In some neurons, T-type Ca^{2+} channels are thought to participate in the generation of low-frequency spiking and high-frequency bursting [20–22]. In either case, rebound action potentials, which are generated by relatively strong hyperpolarization, play an important role [23]. However, GnRH neurons do not show typical bursting activity, in contrast with that observed in magnocellular hypothalamic neurons [24–26]. Indeed, only a single rebound action potential was observed in rat GnRH neurons. During spiking, GnRH neurons hyperpolarize after each action potential or after weak bursting to around −70 mV at most [24–26], which may not deactivate T-type Ca^{2+} channels sufficiently to generate rebound Ca^{2+} spikes. However, the T-type Ca^{2+} channels may be involved in the generation of rhythmic membrane potential oscillations that underlie a tonic or burst firing [27].

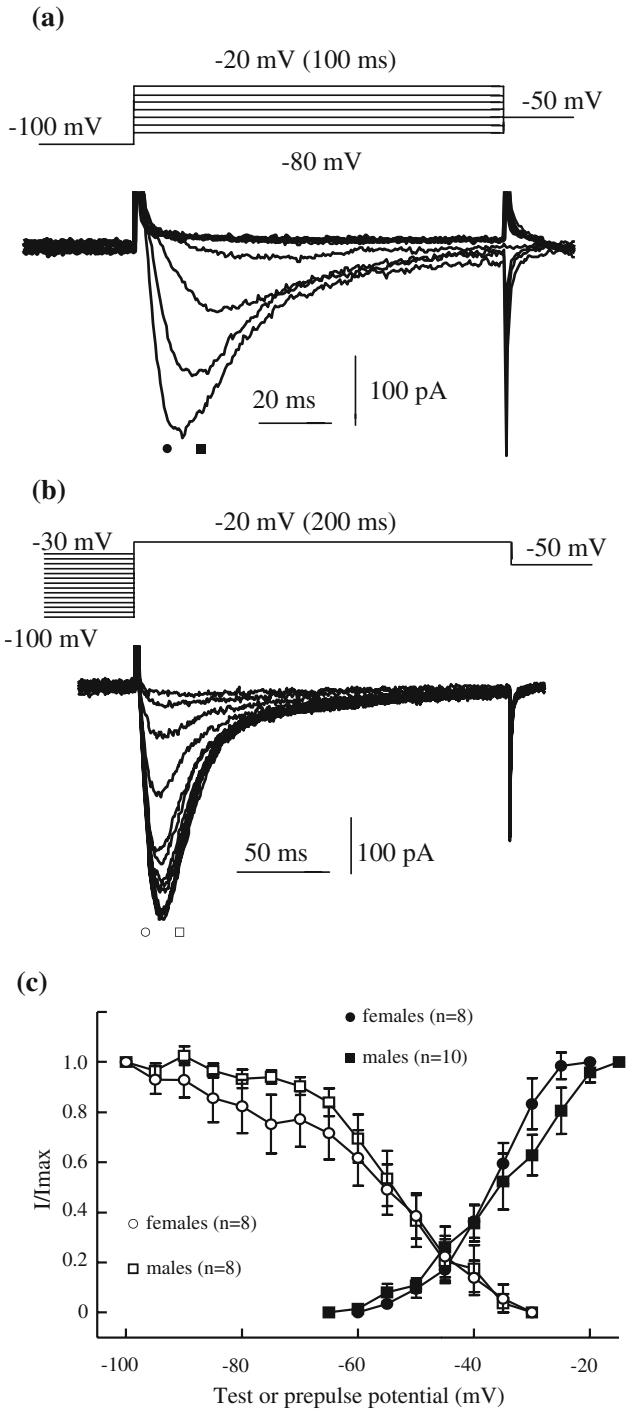

Fig. 4 Activation and steady-state inactivation of T-type Ca^{2+} currents. **a** Test pulses (−80 up to −20 mV) for activation were applied at 0.1 Hz and the peak current at each potential was measured. **b** Two-second prepulses (−100 to −30 mV) were applied at 0.1 Hz, and then the peak current elicited by a test pulse (−20 mV) was measured. **c** Activation and steady-state inactivation are shown. The data were normalized by the value at −20 mV for the activation and by the value at −100 mV for the steady-state inactivation. The activation threshold was −60 mV and full steady-state inactivation was achieved at −30 mV. The half-inactivation voltage was ~−55 mV. Data represent mean ± SEM

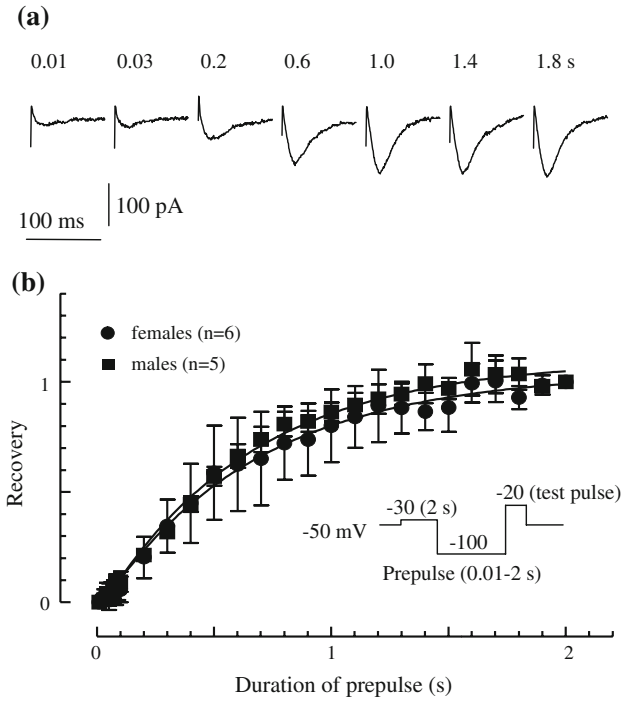

Fig. 5 Recovery time courses of the T-type Ca^{2+} currents in adult rats. The voltage sequence is shown (**b**, *inset*). A 2-s pulse of −30 mV was applied to fully inactivate the T-type Ca^{2+} channels, followed by −100 mV prepulses of variable lengths to deactivate the channels, and finally a 100-ms test pulse of −20 mV was applied. **a** Representative current traces are shown. The *number above each trace* indicates the length of the prepulse. **b** Recovery time courses of the T-type Ca^{2+} currents. The time constants of the recovery were determined by exponential regression analysis of the pooled data for males and females. The time constants were 0.61 s ($n = 6$) for females and 0.54 s ($n = 5$) for males. Data represent mean ± SEM

Therefore, the T-type Ca^{2+} channels seem to function together with SK channels to generate continuous spiking in rat GnRH neurons [2]. On the other hand, dendritic T-type Ca^{2+} channels, together with R-type Ca^{2+} channels, may be involved in the generation of Ca^{2+} spikes [6]. Dendritic Ca^{2+} spikes mainly function for the back propagation of somatic spikes to the entire dendrite [28], which reduces the excitability of the dendritic membrane [29]. Dendritic spikes produced by T and R-type Ca^{2+} channels may also be conveyed orthodromically to the soma when strong depolarization occurs at the distal dendritic membrane [28]. Anti-dromic and ortho-dromic action potentials have been demonstrated in mouse GnRH neurons, in which Na^{+} channels reside in the dendritic membrane [30]. Therefore, rat GnRH neurons are likely to generate dendritic spikes by mainly activating T and R- type Ca^{2+}channels, and possibly Na^{+} channels. In addition, Ca^{2+} influx through the somatodendritic membrane may facilitate autocrine and/or paracrine actions of GnRH that affect the functions of GnRH neurons, as shown in

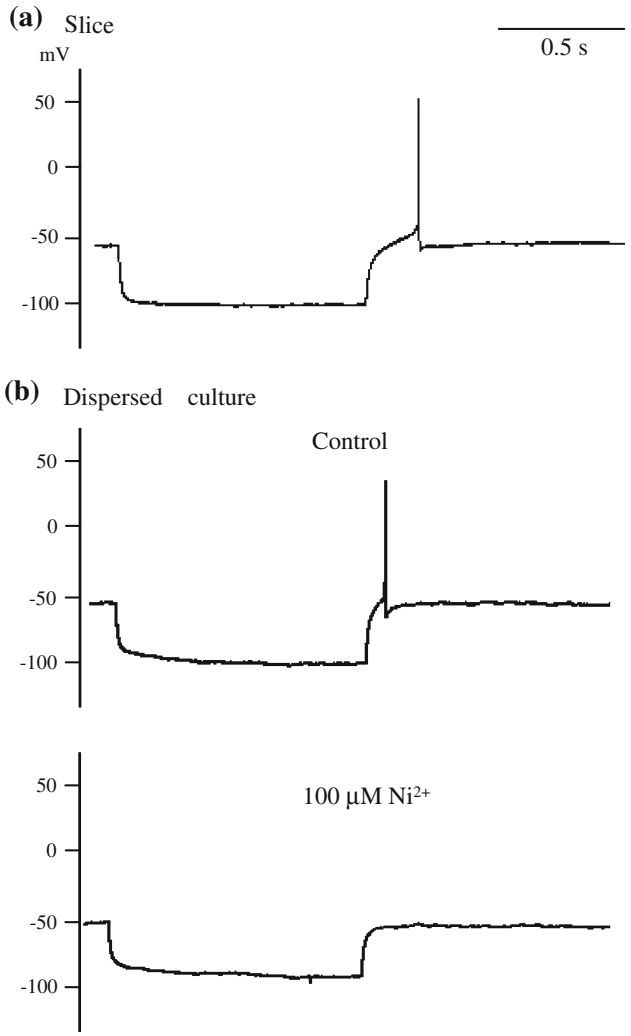

Fig. 6 In current-clamp recordings rebound action potential was generated by 1-s hyperpolarizing current pulse both in GnRH neurons in slice preparation (**a**) and in dispersed GnRH neurons (**b**). The rebound action potential was blocked by 100 μM Ni^{2+}

hypothalamic magnocellular peptidergic neurons [31]. In fact, we have recently shown that ambient GnRH down-regulates the expression of melatonin receptors in GT1-7 cells [32].

In conclusion, rat GnRH neurons express all five types of voltage-gated Ca^{2+} channels. For T-type Ca^{2+} channels, α_{1H} is dominant in adults. There are no sex differences in this expression and no difference with regard to estrous cycle stage for the dominancy of α_{1H} expression.

Acknowledgments We are grateful to Dr Momoko Kobayashi and Ms Sumiko Usui for their technical assistance. This work was supported in part by JSPS Grants-in-Aid for Scientific Research (18590070, 18590226 and 19790181) and MEXT Grants-in-Aid for Scientific Research (16086210 and S0801035).

Conflict of interest statement The authors have nothing to disclose.

References

1. Kato M, Ui-Tei K, Watanabe M, Sakuma Y (2003) Characterization of voltage-gated calcium currents in gonadotropin-releasing hormone neurons tagged with green fluorescent protein in rats. Endocrinology 144:5118–5125
2. Kato M, Tanaka N, Usui S, Sakuma Y (2006) The SK channel blocker apamin inhibits slow afterhyperpolarization currents in rat gonadotropin-releasing hormone neurones. J Physiol 574:431–442
3. Hiraizumi Y, Nishimura I, Ishii H, Tanaka N, Takeshita T, Sakuma Y, Kato M (2008) Rat GnRH neurons exhibit large conductance voltage- and Ca^{2+}-activated K^+ (BK) currents and express BK channel mRNAs. J Physiol Sci 58:21–29
4. Perez-Reyes E (2003) Molecular physiology of low-voltage-activated T-type calcium channels. Physiol Rev 83:117–161
5. Catterall WA, Perez-Reyes E, Snutch TP, Striessnig J (2005) International Union of Pharmacology. XLVIII. Nomenclature and structure-function relationships of voltage-gated calcium channels. Pharmacol Rev 57:411–425
6. Magee JC, Johnston D (1995) Characterization of single voltage-gated Na^+ and Ca^{2+} channels in apical dendrites of rat CA1 pyramidal neurons. J Physiol 487:67–90
7. Nunemaker CS, DeFazio RA, Moenter SM (2003) Calcium current subtypes in GnRH neurons. Biol Reprod 69:1914–1922
8. Spergel DJ (2007) Calcium and small-conductance calcium-activated potassium channels in gonadotropin-releasing hormone neurons before, during, and after puberty. Endocrinology 148:2383–2390
9. Zhang C, Bosch MA, Rick EA, Kelly MJ, Rønnekleiv OK (2009) 17β-estradiol regulation of T-type calcium channels in gonadotropin-releasing hormone neurons. J Neurosci 29:10552–10562
10. Perez-Reyes E, Cribbs LL, Daud A, Lacerda AE, Barclay J, Williamson MP, Fox M, Rees M, Lee JH (1998) Molecular characterization of a neuronal low-voltage-activated T-type calcium channel. Nature 391:896–900
11. Cribbs LL, Lee JH, Yang J, Satin J, Zhang Y, Daud A, Barclay J, Williamson MP, Fox M, Rees M, Perez-Reyes E (1998) Cloning and characterization of α1H from human heart, a member of the T-type Ca^{2+} channel gene family. Circ Res 83:103–109
12. Lee JH, Daud AN, Cribbs LL, Lacerda AE, Pereverzev A, Klockner U, Schneider T, Perez-Reyes E (1999) Cloning and expression of a novel member of the low voltage-activated T-type calcium channel family. J Neurosci 19:1912–1921
13. Lee JH, Gomora JC, Cribbs LL, Perez-Reyes E (1999) Nickel block of three cloned T-type calcium channels: low concentrations selectively block α1H. Biophys J 77:3034–3042
14. Klockner U, Lee JH, Cribbs LL, Daud A, Hescheler J, Pereverzev A, Perez-Reyes E, Schneider T (1999) Comparison of the Ca^{2+} currents induced by expression of three cloned α1 subunits, α1G, α1H and α1I, of low-voltage-activated T-type Ca^{2+} channels. Eur J Neurosci 11:4171–4178
15. McRory JE, Santi CM, Hamming KS, Mezeyova J, Sutton KG, Baillie DL, Stea A, Snutch TP (2001) Molecular and functional characterization of a family of rat brain T-type calcium channels. J Biol Chem 276:3999–4011
16. Tanaka N, Ishii H, Yin C, Sakuma Y, Kato M (2009) T-type Ca^{2+} channels in adult rat gonadotropin-releasing hormone (GnRH) neurons. J Physiol Sci 59(Suppl 1):334 (Abstract)
17. Neher E (1992) Correction for liquid junction potentials in patch clamp experiments. Methods Enzymol 207:123–131
18. Barry PH (1994) JPCalc, a software package for calculating liquid junction potential corrections in patch-clamp, intracellular, epithelial and bilayer measurements and for correcting junction potential measurements. J Neurosci Methods 51:107–116

19. Liu X, Herbison AE (2008) Small-conductance calcium-activated potassium channels control excitability and firing dynamics in gonadotropin-releasing hormone (GnRH) neurons. Endocrinology 149:3598–3604
20. Williams SR, Toth TI, Turner JP, Hughes SW, Crunelli V (1997) The 'window' component of the low threshold Ca^{2+} current produces input signal amplification and bistability in cat and rat thalamocortical neurones. J Physiol 505:689–705
21. Toth TI, Hughes SW, Crunelli V (1998) Analysis and biophysical interpretation of bistable behaviour in thalamocortical neurons. Neuroscience 87:519–523
22. Crunelli V, Toth TI, Cope DW, Blethyn K, Hughes SW (2005) The 'window' T-type calcium current in brain dynamics of different behavioural states. J Physiol 562:121–129
23. Erickson KR, Ronnekleiv OK, Kelly MJ (1993) Role of a T-type calcium current in supporting a depolarizing potential, damped oscillations, and phasic firing in vasopressinergic guinea pig supraoptic neurons. Neuroendocrinology 57:789–800
24. Suter KJ, Wuarin JP, Smith BN, Dudek FE, Moenter SM (2000) Whole-cell recordings from preoptic/hypothalamic slices reveal burst firing in gonadotropin-releasing hormone neurons identified with green fluorescent protein in transgenic mice. Endocrinology 141:3731–3736
25. Sim JA, Skynner MJ, Herbison AE (2001) Heterogeneity in the basic membrane properties of postnatal gonadotropin-releasing hormone neurons in the mouse. J Neurosci 21:1067–1075
26. Kuehl-Kovarik MC, Pouliot WA, Halterman GL, Handa RJ, Dudek FE, Partin KM (2002) Episodic bursting activity and response to excitatory amino acids in acutely dissociated gonadotropin-releasing hormone neurons genetically targeted with green fluorescent protein. J Neurosci 22:2313–2322
27. Bal T, McCormick DA (1993) Mechanisms of oscillatory activity in guinea-pig nucleus reticularis thalami in vitro: a mammalian pacemaker. J Physiol 468:669–691
28. Stuart G, Schiller J, Sakmann B (1997) Action potential initiation and propagation in rat neocortical pyramidal neurons. J Physiol 505:617–632
29. Remy S, Csicsvari J, Beck H (2009) Activity-dependent control of neuronal output by local and global dendritic spike attenuation. Neuron 61:906–916
30. Roberts CB, Campbell RE, Herbison AE, Suter KJ (2008) Dendritic action potential initiation in hypothalamic gonadotropin-releasing hormone neurons. Endocrinology 149:3355–3360
31. Leng G, Ludwig M (2008) Neurotransmitters and peptides: whispered secrets and public announcements. J Physiol 586: 5625–5632
32. Ishii H, Sato S, Yin C, Sakuma Y, Kato M (2009) Cetrorelix, a gonadotropin-releasing hormone antagonist, induces the expression of melatonin receptor 1a in the gonadotropin-releasing hormone neuronal cell line GT1-7. Neuroendocrinology 90:251–259